

Article

Effect of Al (III) Ions on the Separation of Cassiterite and Clinocllore Through Reverse Flotation

Yumeng Chen, Xiong Tong *, Dongxia Feng * and Xian Xie

Faculty of Land Resource Engineering, Kunming University of Science and Technology, Kunming 650093, China; yumengchen0803@126.com (Y.C.); xianxie2008@kmust.edu.cn (X.X.)

* Correspondence: xiongtong2000@yahoo.com (X.T.); dongxia.feng@uqconnect.edu.au (D.F.); Tel.: +86-0871-6551-0286 (X.T. & D.F.)

Received: 16 July 2018; Accepted: 9 August 2018; Published: 11 August 2018



Abstract: Most hydrophobic clay minerals, such as clinocllore, are known to cause problems in the recovery of cassiterite. In this study, a new reagent scheme, i.e., sodium oleate (NaOL) as a collector and Al (III) ions as a depressant, for reverse flotation separation of cassiterite and clinocllore was investigated. The flotation performance and interaction mechanism were studied by microflotation tests, adsorption tests, contact angle measurements, and X-ray photoelectron spectroscopy (XPS) analysis. Results of single mineral flotation experiments showed that NaOL had a different flotation performance on cassiterite and clinocllore, and the addition of Al (III) ions could selectively inhibit the floatability of cassiterite. Reverse flotation tests performed on mixed minerals indicated that the separation of cassiterite and clinocllore could be achieved in the presence of NaOL and Al (III) ions. Adsorption experiments demonstrated that Al (III) ions hindered the adsorption of NaOL on cassiterite surfaces but exerted little influence on the adsorption of NaOL on clinocllore surfaces. Results of contact angle measurements indicated that Al (III) ions could impede the hydrophobization process of cassiterite in NaOL solution. XPS results showed that aluminum species were adsorbed onto the cassiterite surfaces through the interaction with O sites.

Keywords: cassiterite; clinocllore; Al (III) ions; reverse flotation; adsorption

1. Introduction

Tin and its compounds can be applied in many industries, such as soldering, plating, alloy, chemistry, and metallurgy [1]. The global tin resources with industrial utilization value are mainly derived from cassiterite (SnO_2), some of which contain a significant amount of slime (clay mineral) due to overmining [2]. Previous studies [1,3] have indicated that clinocllore is one of the clay minerals encountered in complex tin oxide ores. In industrial utilization, cassiterite should be separated from the clay minerals to improve its purity [1,4,5]. However, with the depletion of cassiterite deposits and decrease of its grade, cassiterite necessitates fine grinding to liberate valuable minerals from low-grade refractory ores. The inherent brittle nature of cassiterite leads to the generation of ultra-fine particles. For fine cassiterite, flotation is an effective method that has been extensively employed for many decades [6–9]. In flotation process, target minerals are separated from gangue minerals, depending on their differences in surface hydrophobicity. Contact angle is a common method to characterize and quantify the surface hydrophobicity [10]. The contact angle of natural cassiterite is around 35° [11], suggesting that the natural hydrophobicity of cassiterite surfaces is very poor. However, clinocllore ($(\text{Mg,Al,Fe})_{12}[(\text{Si,Al})_8\text{O}_{20}](\text{OH})_{16}$) is a layered silicate with 2:1 structure and its contact angle is about 115° in water [12]. It is a hydrophobic clay mineral that can be easily entrained into froth layers, thus lowering the concentrate grade [13,14]. Moreover, clinocllore could attach on cassiterite surfaces as “slime coating”, which has detrimental effect on the recovery of cassiterite in direct flotation even

with an efficient collector [11,15,16]. Therefore, the separation of clinocllore from cassiterite is difficult to achieve in direct flotation due to the hydrophobic property of clinocllore surface.

Reverse flotation has been shown to be an efficient method for de-sliming because the majority of silicates (clay mineral) are hydrophobic minerals [17–20]. Yin et al. [12] reported reverse flotation could be used for removing silicate mineral from hematite with citric acid as a depressant. By using reverse flotation, Wang et al. [18] investigated an economical method that can be used to separate aluminum silicates from diasporic bauxite with quaternary ammonium salt and inorganic reagent. Sodium oleate (NaOL), a fatty acid, is widely used in silicate and oxide minerals flotation. It has shown more advantages in reverse flotation such as lower cost and strong collecting capability [21–24]. However, selective problem arises between cassiterite and clinocllore with NaOL as a collector because of its low selective performance. Therefore, it is crucial that an effective depressant is employed to achieve selective separation [25–28]. There are several studies founding that Al (III) ions can act as a depressant on cassiterite flotation. Zeng et al. [29] and Choi et al. [30] studied the effects of metal ions on cassiterite flotation with sulphosuccinamate as a collector and they both found that Al (III) ions could inhibit the floatability of cassiterite. However, no one has reported the effect of Al (III) ions on the floatability of cassiterite when NaOL is used as a collector.

The objective of this study is to determine whether clinocllore can be efficiently separated from cassiterite in the presence of NaOL and Al (III) ions through reverse flotation. Microflotation tests of single and mixed minerals were conducted to examine the selective separation behavior. Adsorption tests were performed to analyze the influence of Al (III) ions on the adsorbed amount of NaOL under different mineral surfaces. Contact angle measurements were implemented using the bubble method to study the effect of Al (III) ions on the hydrophobization process of cassiterite in NaOL solution. X-ray photoelectron spectroscopy (XPS) analyses were employed to reveal the adsorption mechanism of Al (III) ions and cassiterite surfaces. With the combinations of fatty acid and cations, the results provide a basis for effective separation of oxide mineral and silicate mineral using reverse flotation.

2. Materials and Methods

2.1. Materials

Pure cassiterite and clinocllore were obtained from the YiLiang deposits in China and Kawaii deposits in Russia, respectively. The X-ray powder diffraction (XRD) patterns of them were illustrated in Figure 1, confirming the purity of the two minerals. The bulk crystals of cassiterite were polished to form a flat surface, which was later cleaned and used for contact angle measurements. Some mineral samples of cassiterite and clinocllore were both artificially crushed and ground using an agate mortar. After sieving, the fraction with a particle size of $-39\ \mu\text{m}$ was used for microflotation experiments and adsorption experiments. Moreover, parts of cassiterite samples were further fine ground to $-5\ \mu\text{m}$ for XPS analyses.

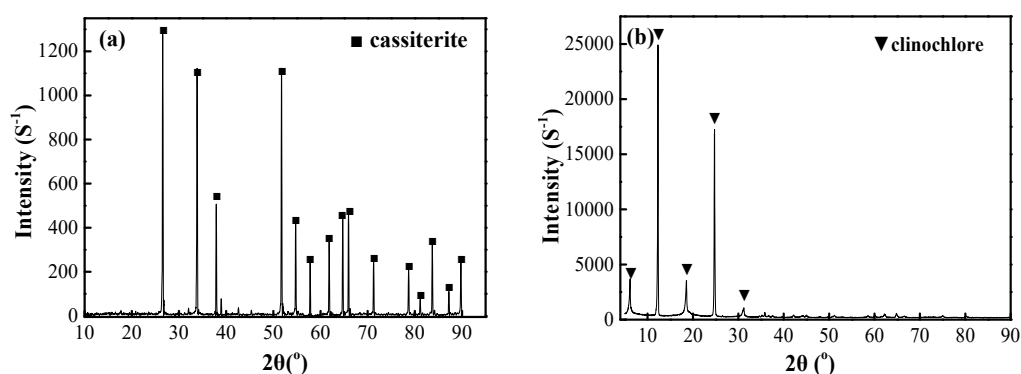


Figure 1. X-ray powder diffraction (XRD) patterns of samples: (a) cassiterite; (b) clinocllore.

Sodium oleate (NaOL) used as a collector and aluminum sulfate ($\text{Al}_2(\text{SO}_4)_3 \cdot 18\text{H}_2\text{O}$) used as a depressant were both purchased from Chemical Research Institute, Tianjin, China. Hydrochloric acid (HCl) and sodium hydroxide (NaOH) were used to adjust the pH values. Fresh deionized water, with electrical resistivity $>0.18 \text{ M}\Omega\text{m}$, was used in all experiments.

2.2. Methods

2.2.1. Flotation Tests

The microflotation tests were performed using a 50 dm^3 cell (XFG II). The impeller speed was fixed at 1800 rpm. The microflotation tests involved three groups of tests. Flotation tests of single mineral were conducted within different concentrations of NaOL and pH values, and the optimum condition of NaOL dosage and pH value was determined. Then, microflotation tests of single mineral within different concentrations of Al (III) ions were carried out under this condition. Finally, flotation tests of binary mixed minerals (1 g cassiterite plus 1 g clinocllore) were proceeded to further study the depressive performance of Al (III) ions. In each test, 2 g of sample was placed into the cell with 50 dm^3 deionized water, and the pulp was stirred for 1 min to obtain mineral suspension. The pH value of pulp was adjusted by adding pH regulators and agitating for 3 min. After each of the desired reagents was added, the suspension was agitated for 3 min. The flotation time was 2 min and the concentrate was collected by manually scraping. For single mineral flotation, the collected concentrates were filtered, dried and weighed for calculating flotation recovery. For binary mixed mineral flotation tests, the products of unfloted particles were filtered, dried and weighed. The Sn grades of the unfloted particles were assayed and were used for calculating the recoveries.

2.2.2. Adsorption Tests

The adsorption tests of NaOL on the minerals surfaces treated and not treated with Al (III) ions were conducted in a thermostatic water bath at 298 K. Minerals samples (2 g) were dispersed into 50 dm^3 of aqueous phase in the absence and presence of $3 \times 10^{-4} \text{ mol/dm}^3$ Al (III) ions. After the mineral suspensions were conditioned for 30 min, the NaOL solution of a desired concentration was injected to interact with the mineral surface, and the mixture was stirred for another 30 min. The resultant suspension was immediately subjected to solid–liquid separation by a centrifuge, and the separated liquid was collected to quantitatively analyze the NaOL concentration using a UV-Vis spectrophotometer (UV-2700, Shimadzu, Kyoto, Japan) at a wavelength of 230 nm. Each test was repeated three times and the average adsorbed amount was reported. The adsorbed amount of NaOL on the minerals surfaces was calculated using the following equation:

$$\Gamma = \frac{(C_0 - C)V}{m} \quad (1)$$

where C_0 and C are the initial and supernatant concentrations of NaOL in the solution, respectively. V is the volume of flotation solution, and m is the weight of mineral.

2.2.3. Contact Angle Measurements

Contact angle measurements were implemented using the bubble method. Three groups of measurements were performed with water, NaOL solution ($5 \times 10^{-5} \text{ mol/dm}^3$) and Al (III) ions & NaOL solution (3×10^{-4} & $5 \times 10^{-5} \text{ mol/dm}^3$), respectively. The cassiterite samples were treated for 30 min in designated solutions. Then the treated sample was placed on two stable supports with the polished surface facing downward in a rectangular glass chamber which was filled with the desired solution. A small bubble was produced by special equipment, which consisted of a unique U-shaped needle and a microsyringe. The bubble was then released from the needle tip at a fixed distance (0.8 cm) below the submerged specimen surface. Buoyancy forces could drive the bubble to the mineral surface. After the air bubble attached to the solid surface, images were recorded by a microscopic

camera. The contact angle was calculated automatically after processing the images in MATLAB (The MathWorks Inc., Natick, MA, USA). This procedure was repeated 10 times for each set of solution.

2.2.4. XPS Analysis

The XPS analyses were recorded on a PHI5000 Versa Probe II (PHI5000, ULVAC-PHI, Hagisono, Japan) with an Al K α X-ray source. A survey scan of the samples was first conducted to detect elemental compositions, and then high-resolution scans were used to measure the elements of Al, Sn and O. All spectra were calibrated according to the C1s spectrum at binding energy of 284.80 eV for charge compensation. The MultiPak spectrum software (Version 9.0) was used to calculate and analyze the results. XPS analyses included two cassiterite samples, i.e., pure cassiterite and cassiterite treated with Al (III) ions. The treated cassiterite sample was prepared by adding 2 g cassiterite into 50 dm³ Al (III) ions solution (3×10^{-4} mol/dm³) and agitated for 30 min. The sample were collected, dried, and stored for XPS analyses.

3. Results and Discussion

3.1. Flotation Tests

To explore preferred the NaOL dosage and pH, a series of single mineral flotation experiments are conducted for separation of cassiterite and clinochlore. As shown in Figure 2a, the floatability of cassiterite is lower than that of clinochlore as the NaOL concentration rises from 2×10^{-5} mol/dm³ to 8×10^{-5} mol/dm³. It is exciting to note that the recovery of clinochlore rises with the increase of NaOL concentration. The flotation recovery of cassiterite increases gradually with increase of the NaOL concentration under 5×10^{-5} mol/dm³. When the concentration of NaOL is greater than 5×10^{-5} mol/dm³, the flotation recovery of cassiterite increases rapidly. The biggest gap between the recoveries of cassiterite and clinochlore appears at around 5×10^{-5} mol/dm³ NaOL, indicating that it has the best separation effect. Figure 2b shows the recoveries of cassiterite and clinochlore as a function of pH under 5×10^{-5} mol/dm³ NaOL. The recoveries of cassiterite and clinochlore increases with increasing pH, but decrease as pH values exceed 8.0. Thus, the optimum condition for separation of cassiterite and clinochlore is 5×10^{-5} mol/dm³ NaOL solution at pH 8.0. In what follows, flotation tests were performed under this condition to explore the effects of Al (III) ions concentration on the separation of clinochlore from cassiterite by reverse flotation.

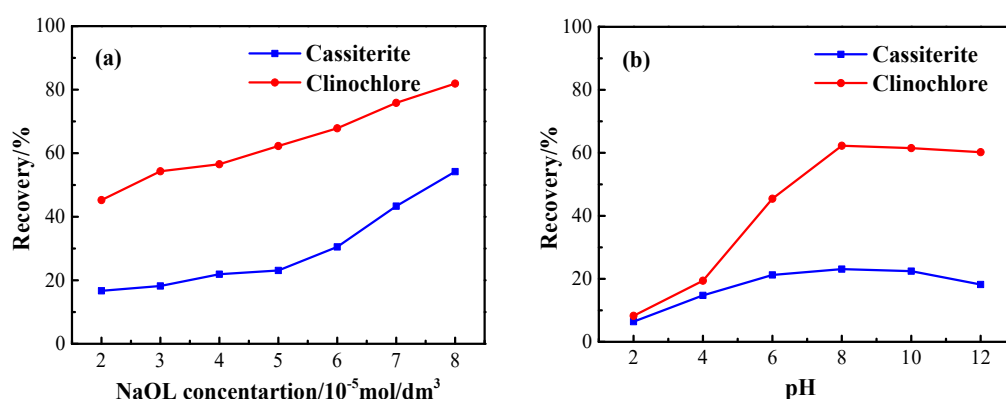
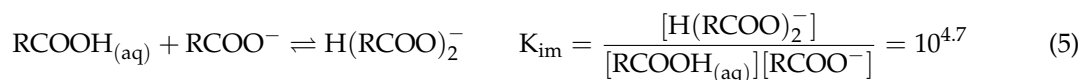
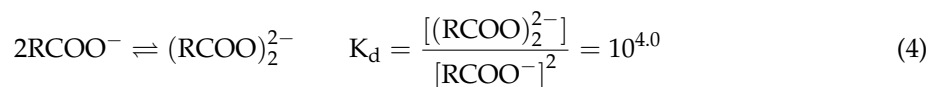
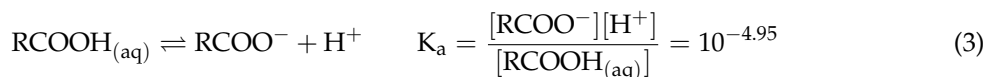


Figure 2. Effect of (a) NaOL concentration (at pH 8.0) and (b) pH values (at NaOL concentration of 5×10^{-5} mol/dm³) on floatability of cassiterite and clinochlore.

Sodium oleate can be dissociated and hydrolyzed in the pulp solution [31,32]. The corresponding chemical reactions and equilibrium constants are shown as follows:





According to Equations (2)–(5), the species distribution diagrams of sodium oleate are shown in Figure 3, which help to explain the results obtained from flotation experiments. As shown in Figure 3, the distribution of oleate species in the pulp solution is greatly determined by the value of pH. At acidic pH, the RCOOH molecules are difficult to dissociate due to the existence of numerous H^+ ions in aqueous solutions. Thus sodium oleate will be mainly present in the form of molecule (i.e., oleic acid). The concentration of OH^- ions increases and parts of RCOOH molecules are dissociated into RCOO^- (i.e., oleate ions) with increasing pH of the aqueous solution. The generated RCOO^- ions will be associated with other RCOO^- ions to form $(\text{RCOO})_2^{2-}$ (i.e., oleate dimers) and also associated with RCOOH molecules to produce $\text{H}(\text{RCOO})_2^-$ (i.e., acid-soap complex). At alkaline pH, oleate ions and oleate dimers are the primary species of sodium oleate in the pulp solution. Based on the results in Figure 2b, the lower flotation recovery at acidic pH may be attributed to the low concentration of oleate ions. The specie of oleic acid disappears at pH 8.1, which causes the decrease of flotation recovery at alkaline pH. In addition, cassiterite and clinochlore cannot be well floated under strong alkaline condition due to the competitive adsorption of hydroxyl ions with oleate species (RCOO^- and $(\text{RCOO})_2^{2-}$) [32].

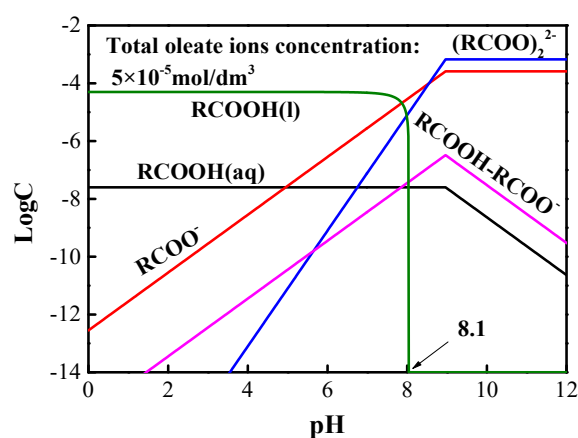


Figure 3. Effect of pH on species distribution diagrams of sodium oleate at concentration of $5.0 \times 10^{-5} \text{ mol/dm}^3$.

Figure 4a shows the recoveries of cassiterite and clinochlore conditioned with different Al (III) ions concentrations. The recovery of cassiterite decreases as Al (III) ions concentration increase. In contrast, a slight increase in recovery of clinochlore is observed within increasing Al (III) ions concentration. The aggregation of the fine clinochlore particles caused by aluminum sulfate increases the probability of collision with the bubble, which is reflected in increased flotation recovery [33,34]. Especially, at Al (III) ions concentration above $2.4 \times 10^{-4} \text{ mol/dm}^3$, the recovery of cassiterite is below 10% while that of clinochlore remains above 70%. This finding, which is in good agreement with previous studies [29,30], demonstrates that Al (III) ions inhibit the floatability of cassiterite. The effect of pH on the flotation recoveries of cassiterite and clinochlore in the presence of $2.4 \times 10^{-4} \text{ mol/dm}^3$ Al (III) ions using NaOL as a collector is shown in Figure 4b. With the increase of pH from 2 to 8, the flotation recovery of clinochlore increases from 10% to 70%, and then it turns to decrease to 40% at pH 12. However, the pH

has a small effect on floatability of cassiterite because the flotation recovery of cassiterite is below 10% across the entire pH range. Hence, it can be seen that the preferable pH value for flotation separation of cassiterite and clinochlore is 8.0 with Al (III) ions as a depressant.

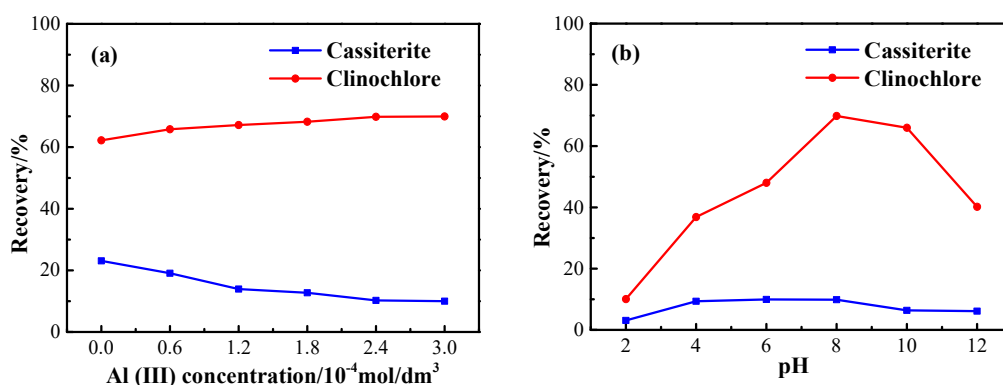


Figure 4. Effect of (a) Al (III) ions concentration (at pH 8.0) and (b) pH values (at Al (III) ions concentration of $2.4 \times 10^{-4} \text{ mol/dm}^3$) on floatability of cassiterite and clinochlore.

In order to determine whether cassiterite could be separated from clinochlore with Al (III) ions as a depressant, cassiterite and clinochlore are mixed by 1:1 (mass ratio) and floated at pH 8.0 using NaOL as a collector. The effect of Al (III) ions concentration on the Sn grade and recovery of unfloated particles are plotted in Figure 5. The Sn grade and the recovery of unfloated particles both increase continuously when the concentration of Al (III) ions is less $3 \times 10^{-4} \text{ mol/dm}^3$. By using a depressant with $3 \times 10^{-4} \text{ mol/dm}^3$ Al (III) ions and a collector with $5 \times 10^{-5} \text{ mol/dm}^3$ NaOL, the unfloated particles with Sn grade of 64% and recovery of 88% are obtained. These results illustrate that the separation of cassiterite and clinochlore could be achieved with Al (III) ions as a depressant by reverse flotation, and the loss of cassiterite recovery is only about 12% in froth.

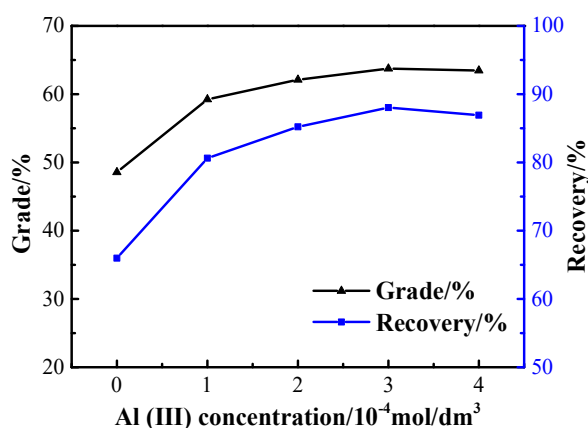


Figure 5. Effect of Al (III) ions concentration on Sn grade and recovery of unfloated particles (at pH 8.0 and NaOL concentration of $5 \times 10^{-5} \text{ mol/dm}^3$).

3.2. Adsorption Tests

In order to ascertain the contribution of Al (III) ions to the adsorbed amount of NaOL on the minerals surfaces and the implications for the flotation separation of cassiterite and clinochlore, the adsorption behaviors of NaOL on the mineral surface treated with and without Al (III) ions are investigated. Figure 6 shows the adsorbed amount of NaOL on the cassiterite and clinochlore surfaces as a function of NaOL concentration in the absence and presence of Al (III) ions. The adsorbed amount of NaOL on the minerals surfaces gradually increases with an increase in collector concentration.

As shown in Figure 6a, the adsorbed amount of NaOL on the cassiterite surfaces treated with Al (III) ions is lower than that of bare cassiterite surfaces. Figure 6b shows that the adsorbed amounts of NaOL on clinoclhore surfaces have no significant difference between the two groups before and after Al (III) ions treatment. This finding indicates that the adsorbed amount of NaOL on cassiterite surfaces is decreased with the addition of Al (III) ions solution, while no changes are found on clinoclhore surfaces.

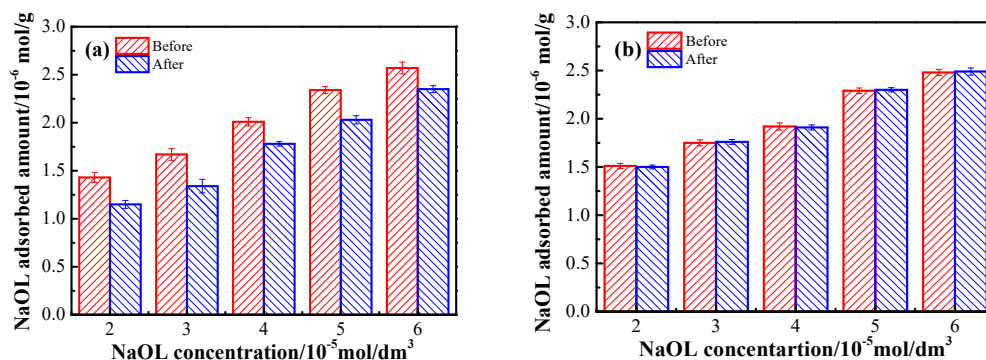


Figure 6. Effect of NaOL concentration on the adsorbed amount of NaOL on minerals surfaces in the absence and presence of Al (III) ions (at pH 8.0): (a) cassiterite surfaces; (b) clinoclhore surfaces.

As shown in Figure 7, the distribution diagram of aluminum species is calculated using Visual MINTEQ 3.1 software (KTH, Stockholm, Sweden), as the function of pH at the concentration of 3.0×10^{-4} mol/dm³. The solution contains various aluminum species, of which $\text{Al}(\text{OH})_4^-$ is the main species at pH 8.0. In addition, its concentration reaches 2.81×10^{-4} mol/dm³ in aqueous solutions. Figures 6a and 7 signify that hydrated $\text{Al}(\text{OH})_4^-$ is adsorbed onto the cassiterite surfaces, which hinders the adsorption of oleate species onto the cassiterite surfaces, thereby weakening the hydrophobicity of cassiterite and decreasing its floatability.

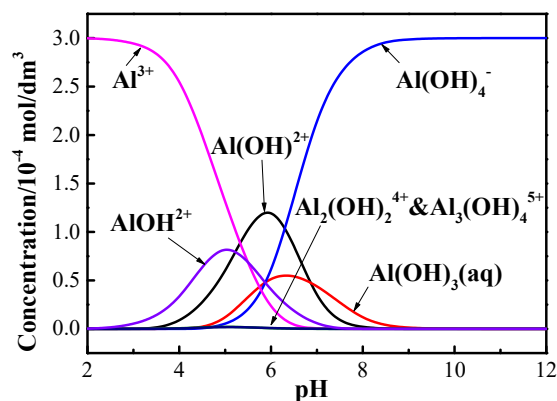


Figure 7. Effect of pH on species distribution diagrams of Al (III) ions at concentration of 3.0×10^{-4} mol/dm³.

3.3. Contact Angle Measurements

Contact angles of cassiterite in different solutions are demonstrated in Figure 8. As shown in Figure 8a, the contact angle of cassiterite in water is around 34° , indicating a weak hydrophobicity. After being treated with 5×10^{-5} mol/dm³ NaOL, the contact angle increases to about 54° (Figure 8b), which signifies that the adsorption of NaOL on cassiterite surface could enhance the hydrophobicity. Figure 8c shows that the contact angle of cassiterite surface is approximately 45° in 3×10^{-4} mol/dm³ Al (III) ions and 5×10^{-5} mol/dm³ NaOL solution, thus indicating that Al (III) ions weaken the hydrophobization process of cassiterite in NaOL solution. Compared with the results of adsorption

tests, there is a significant decrease in contact angle of cassiterite surface after the addition of Al (III) ions. Meanwhile, the decreasing tendency agrees well with the microflotation findings.

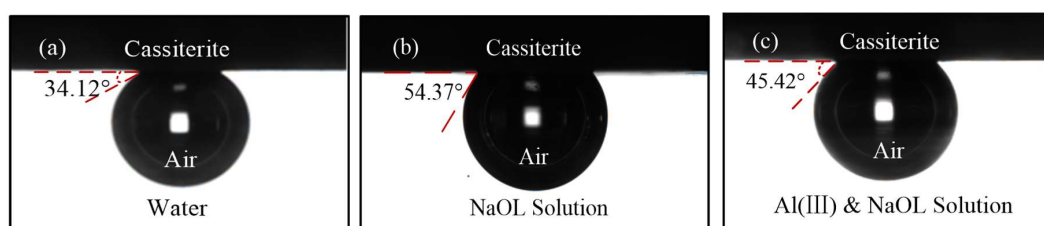


Figure 8. The contact angle of cassiterite in different solutions: (a) water; (b) sodium oleate solution of $5 \times 10^{-5} \text{ mol/dm}^3$; (c) mixture of Al (III) ions and sodium oleate solution ($3 \times 10^{-4} \text{ mol/dm}^3$ and $5 \times 10^{-5} \text{ mol/dm}^3$, respectively).

3.4. XPS Analysis

XPS measurements are applied to further reveal the effect of Al (III) ions on surface properties of cassiterite. Figure 9 gives the elements identified by the XPS analysis on cassiterite surfaces. It demonstrates that after Al (III) ions adsorption, the atomic concentration of O increases and that of Sn decreases, and the signal of Al is detected with an atomic concentration of 3.3%. Hence, the elemental composition of the cassiterite surfaces changes and a new specie appears after Al (III) ions treatment. This phenomenon implies indicate that the Al (III) ions may be attached on the cassiterite surfaces via adsorption, precipitation, or a combination of the two.

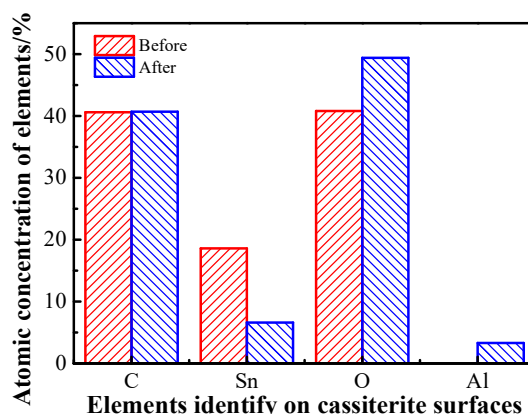


Figure 9. Atomic concentration of elements for the cassiterite surfaces before and after Al (III) ions treatment as determined by XPS.

The high-resolution XPS spectra of the cassiterite surfaces are presented in Figure 10. As shown in Figure 10a₁, a signal of Al is not detected on pure cassiterite surface. A new, weak peak appears at 74.76 eV in the XPS spectra of cassiterite treated with Al (III) ions (Figure 10b₁). The binding energy of Al2p in the standard spectra of Al is reported as 72.80 eV [35], but the peak of Al in cassiterite surfaces is at 74.76 eV. This phenomenon may be attributed to hydrated $\text{Al}(\text{OH})_4^-$, which is the main species at pH 8.0. Figure 10a₂ displays that Sn3d XPS spectra of pure cassiterite are well fitted by two spin-orbit split peaks, with binding energies of 494.75 eV for the Sn3d3/2 level and 486.26 eV for the Sn3d5/2 level, respectively [36]. After Al (III) ions treatment, almost no changes are found in the binding energy of Sn3d spectra (Figure 10b₂). It indicates that Sn sites on the cassiterite surfaces exhibit very weak reactivity towards the adsorption of Al (III) ions. Figure 10a₃ shows that O1s XPS peaks of pure cassiterite are composed of two components, 531.64 eV for Sn–O and 530.19 eV for O–H [37]. As shown in Figure 10b₃, after the treatment with Al (III) ions, they slightly shift to greater values

at 532.03 eV and 530.45 eV, resulting from the increase in electron cloud density [38]. These findings indicate that aluminum species in the form of $\text{Al}(\text{OH})_4^-$ are adsorbed onto the cassiterite surfaces through the interaction with O sites.

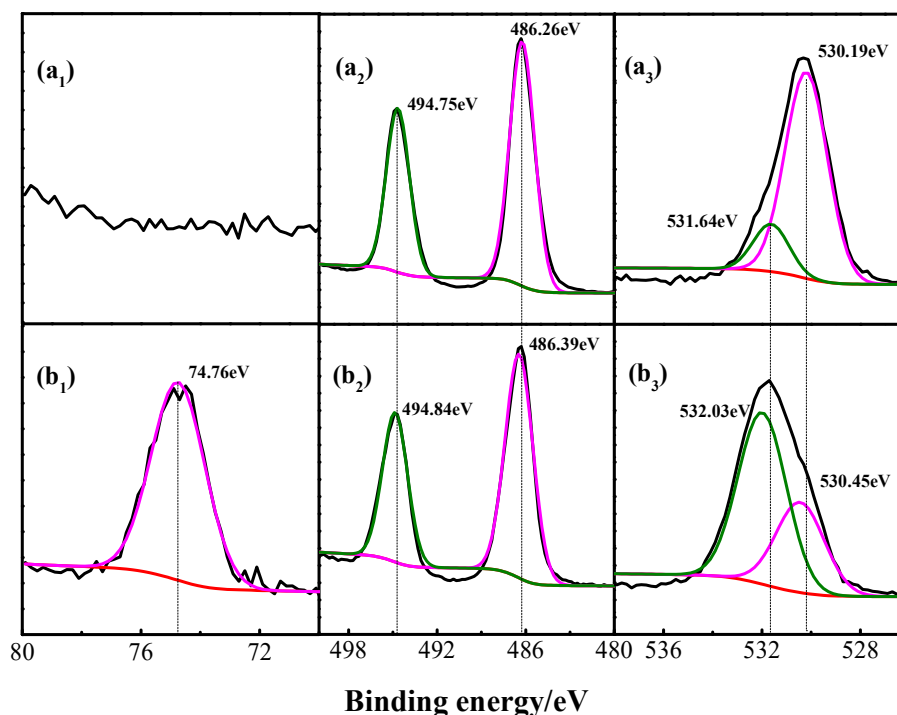


Figure 10. XPS spectra on the cassiterite surfaces: (a₁) Al2p peaks of pure cassiterite; (b₁) Al2p peaks of cassiterite treated with Al (III) ions; (a₂) Sn3d peaks of pure cassiterite; (b₂) Sn3d peaks of cassiterite treated with Al (III) ions; (a₃) O1s peaks of pure cassiterite; (b₃) O1s peaks of cassiterite treated with Al (III) ions.

4. Conclusions

This work investigated the effects of Al (III) ions on the adsorption of NaOL onto cassiterite and clinocllore surfaces and the implications for their separation by reverse flotation. Flotation tests of single mineral indicated that there was an obvious floatability difference for cassiterite and clinocllore by using NaOL as a collector, and the gap could be enhanced in presence of Al (III) ions. The results of artificially mixed minerals flotation further demonstrated that Al (III) ions can separate clinocllore from cassiterite through reverse flotation, and the loss of cassiterite recovery was only about 12% in froth. Adsorption tests showed that the addition of Al (III) ions could decrease the adsorption amount of NaOL on the cassiterite surfaces, while there was no decreasing phenomenon on clinocllore surfaces. Contact angle measurements verified Al (III) ions hindered the adsorption of NaOL on cassiterite surfaces. XPS analyses revealed that Al (III) ions were adsorbed onto the cassiterite surfaces through the interaction with the O sites. This study provides a fundamental understanding of Al (III) ions behavior in cassiterite flotation with NaOL as a collector. It is of great significance to use this depression effect to remove clinocllore from cassiterite through reverse flotation.

Author Contributions: Y.C. and X.T. conceived and designed the experiments; Y.C. and D.F. performed the experiments and analyzed the data; X.T. and X.X. contributed reagents and materials; Y.C. and X.T. wrote the paper.

Funding: This research was supported by the National Natural Science Foundation of China (51764024).

Acknowledgments: We sincerely thank Jinfang Lv and Zhongbao Hua for their important guidance and assistant in flotation experiments.

Conflicts of Interest: The authors declare no conflicts of interest.

References

1. Angadi, S.I.; Sreenivas, T.; Jeon, H.S.; Baek, S.H.; Mishra, B.K. A review of cassiterite beneficiation fundamentals and plant practices. *Miner. Eng.* **2015**, *70*, 178–200. [[CrossRef](#)]
2. Tian, M.; Liu, R.; Gao, Z.; Chen, P.; Han, H.; Wang, L.; Zhang, C.; Sun, W.; Hu, Y. Activation mechanism of Fe (III) ions in cassiterite flotation with benzohydroxamic acid collector. *Miner. Eng.* **2018**, *119*, 31–37. [[CrossRef](#)]
3. Liao, Z.; Liu, Y.P.; Li, C.Y. Characteristics of chlorites from dulong Sn-Zn deposit and their metallogenic implications. *Miner. Deposit.* **2010**, *29*, 169–176.
4. Edwards, C.R.; Kipkie, W.B.; Agar, G.E. The effect of slime coatings of the serpentine minerals, chrysotile and lizardite, on pentlandite flotation. *Int. J. Miner. Process.* **1980**, *7*, 33–42. [[CrossRef](#)]
5. Peng, Y.; Zhao, S. The effect of surface oxidation of copper sulfide minerals on clay slime coating in flotation. *Miner. Eng.* **2011**, *24*, 1687–1693. [[CrossRef](#)]
6. Wu, X.Q.; Zhu, J.G. Selective flotation of cassiterite with benzohydroxamic acid. *Miner. Eng.* **2006**, *19*, 1410–1417. [[CrossRef](#)]
7. Cheng, T.W.; Holtham, P.N.; Tran, T. Froth flotation of monazite and xenotime. *Miner. Eng.* **1993**, *6*, 341–351. [[CrossRef](#)]
8. Leistner, T.; Embrechts, M.; Leibner, T.; Chelgani, S.C.; Osbahr, I.; Möckel, R.; Peuker, U.A.; Rudolph, M. A study of the reprocessing of fine and ultrafine cassiterite from gravity tailing residues by using various flotation techniques. *Miner. Eng.* **2016**, *96–97*, 94–98. [[CrossRef](#)]
9. Xing, Y.; Gui, X.; Pan, L.; Pinchasik, B.E.; Cao, Y.; Liu, J.; Kappl, M.; Butt, H.J. Recent experimental advances for understanding bubble-particle attachment in flotation. *Adv. Colloid Interface Sci.* **2017**, *246*, 105–132. [[CrossRef](#)] [[PubMed](#)]
10. Chau, T.T. A review of techniques for measurement of contact angles and their applicability on mineral surfaces. *Miner. Eng.* **2009**, *22*, 213–219. [[CrossRef](#)]
11. Ren, L.; Qiu, H.; Zhang, M.; Feng, K.; Liu, P.; Guo, J.; Feng, J. The behavior of lead ions in cassiterite flotation using octanohydroxamic acid. *Ind. Eng. Chem. Res.* **2017**, *56*, 8723–8728. [[CrossRef](#)]
12. Yin, W.; Fu, Y.; Yao, J.; Yang, B.; Cao, S.; Sun, Q. Study on the dispersion mechanism of citric acid on chlorite in hematite reverse flotation system. *Minerals* **2017**, *7*, 221.
13. Zheng, G.S.; Liu, L.J.; Liu, J.T.; Wang, Y.T.; Cao, Y.J. Study of chlorite flotation and its influencing factors. *Procedia Earth. Planetary Sci.* **2009**, *1*, 830–837.
14. Neethling, S.J.; Cilliers, J.J. The entrainment of gangue into a flotation froth. *Int. J. Miner. Process.* **2002**, *64*, 123–134. [[CrossRef](#)]
15. Yu, Y.; Ma, L.; Cao, M.; Liu, Q. Slime coatings in froth flotation: A review. *Miner. Eng.* **2017**, *114*, 26–36. [[CrossRef](#)]
16. Feng, Q.; Zhao, W.; Wen, S.; Cao, Q. Activation mechanism of lead ions in cassiterite flotation with salicylhydroxamic acid as collector. *Sep. Purif. Technol.* **2017**, *178*, 193–199. [[CrossRef](#)]
17. Shrimali, K.; Atluri, V.; Wang, Y.; Bacchuwar, S.; Wang, X.; Miller, J.D. The nature of hematite depression with corn starch in the reverse flotation of iron ore. *J. Colloid Interface Sci.* **2018**, *524*, 337–349. [[CrossRef](#)] [[PubMed](#)]
18. Wang, Y.; Hu, Y.; He, P.; Gu, G. Reverse flotation for removal of silicates from diasporic-bauxite. *Miner. Eng.* **2004**, *17*, 63–68. [[CrossRef](#)]
19. Yao, J.; Yin, W.; Gong, E. Depressing effect of fine hydrophilic particles on magnesite reverse flotation. *Int. J. Miner. Process.* **2016**, *149*, 84–93. [[CrossRef](#)]
20. Xing, Y.; Xu, M.; Gui, X.; Cao, Y.; Babel, B.; Rudolph, M.; Weber, S.; Kappl, M.; Butt, H.J. The application of atomic force microscopy in mineral flotation. *Adv. Colloid Interface Sci.* **2018**, *256*, 373–392. [[CrossRef](#)] [[PubMed](#)]
21. Li, H.; Liu, M.; Liu, Q. The effect of non-polar oil on fine hematite flocculation and flotation using sodium oleate or hydroxamic acids as a collector. *Miner. Eng.* **2018**, *119*, 105–115. [[CrossRef](#)]

22. Roonasi, P.; Yang, X.; Holmgren, A. Competition between sodium oleate and sodium silicate for a silicate/oleate modified magnetite surface studied by in situ atr-ftir spectroscopy. *J. Colloid Interface Sci.* **2010**, *343*, 546–552. [[CrossRef](#)] [[PubMed](#)]
23. Xu, Y.; Qin, W. Surface analysis of cassiterite with sodium oleate in aqueous solution. *Sep. Sci. Technol.* **2012**, *47*, 502–506. [[CrossRef](#)]
24. Liu, J.; Gong, G.; Han, Y.; Zhu, Y. New insights into the adsorption of oleate on cassiterite: A DFT study. *Minerals* **2017**, *7*, 236. [[CrossRef](#)]
25. Schubert, H.; Schoenherr, J.; Schubert, H. Alkane dicarboxylic acids and aminonaphthol-sulfonic acids—A new reagent regime for cassiterite flotation. *Int. J. Miner. Process.* **1985**, *15*, 117–133.
26. Tian, M.; Gao, Z.; Han, H.; Sun, W.; Hu, Y. Improved flotation separation of cassiterite from calcite using a mixture of lead (ii) ion/benzohydroxamic acid as collector and carboxymethyl cellulose as depressant. *Miner. Eng.* **2017**, *113*, 68–70. [[CrossRef](#)]
27. Ren, Z.; Yu, F.; Gao, H.; Chen, Z.; Peng, Y.; Liu, L. Selective separation of fluorite, barite and calcite with valonea extract and sodium fluosilicate as depressants. *Minerals* **2017**, *7*, 24. [[CrossRef](#)]
28. Gao, Y.; Gao, Z.; Sun, W.; Hu, Y. Selective flotation of scheelite from calcite: A novel reagent scheme. *Int. J. Miner. Process.* **2016**, *154*, 10–15. [[CrossRef](#)]
29. Zeng, Q.; Hong, Z.; Wang, D. Influence of metal cations on cassiterite flotation. *Trans. Nonferr. Metal. Soc.* **2000**, *10*, 98–101.
30. Choi, W.; Zeng, Q.; Jiang, E.; SeokJeon, H. Cassiterite flotation with sulphosuccinamate collector. *Geosyst. Eng.* **1998**, *1*, 30–34. [[CrossRef](#)]
31. Quast, K. Literature review on the interaction of oleate with non-sulphide minerals using zeta potential. *Miner. Eng.* **2016**, *94*, 10–20. [[CrossRef](#)]
32. Feng, Q.; Wen, S.; Zhao, W.; Chen, Y. Effect of calcium ions on adsorption of sodium oleate onto cassiterite and quartz surfaces and implications for their flotation separation. *Sep. Purif. Technol.* **2018**, *200*, 300–306. [[CrossRef](#)]
33. Liu, C.; Chen, Y.; Song, S.; Li, H. The effect of aluminum ions on the flotation separation of pentlandite from lizardite. *Colloid Surf. A-Physicochem. Eng. Asp.* **2018**, in press. [[CrossRef](#)]
34. Medeiros, A.R.S.D.; Baltar, C.A.M. Importance of collector chain length in flotation of fine particles. *Miner. Eng.* **2018**, *122*, 179–184. [[CrossRef](#)]
35. Hauert, R.; Patscheider, J.; Tobler, M.; Zehring, R. XPS investigation of the a-C: H/Al interface. *Surf. Sci.* **1993**, *292*, 121–129. [[CrossRef](#)]
36. Li, F.; Zhong, H.; Zhao, G.; Wang, S.; Liu, G. Flotation performances and adsorption mechanism of α -hydroxyoctyl phosphinic acid to cassiterite. *Appl. Surf. Sci.* **2015**, *353*, 856–864. [[CrossRef](#)]
37. Nowak, P.; Laajalehto, K.; Kartio, I. A flotation related X-ray photoelectron spectroscopy study of the oxidation of galena surface. *Colloid Surf. A-Physicochem. Eng. Asp.* **2000**, *161*, 447–460. [[CrossRef](#)]
38. Tian, M.; Zhang, C.; Han, H.; Liu, R.; Gao, Z.; Chen, P.; He, J.; Hu, Y.; Sun, W.; Yuan, D. Novel insights into adsorption mechanism of benzohydroxamic acid on lead (II)-activated cassiterite surface: An integrated experimental and computational study. *Miner. Eng.* **2018**, *122*, 327–338. [[CrossRef](#)]

